LBL-15684
Preprint

Lawrence Berkeley Laboratory
UNIVERSITY OF CALIFORNIA

Submitted to Zeitschrift für Physik

MEASUREMENTS OF n-p CORRELATIONS IN THE REACTION OF RELATIVISTIC NEON WITH URANIUM

K. Frankel, W. Schimmerling, J.O. Rasmussen,
K.M. Crowe, J. Bistirlich, H. Bowman,
O. Hashimoto, D.L. Murphy, J. Ridout,
J.P. Sullivan, E. Yoo, W.J. McDonald,
M. Salomon, and J.-S. Xu

April 1985

NUCLEAR SCIENCE DIVISION

Prepared for the U.S. Department of Energy under Contract DE-AC03-76SF00098

DISCLAIMER

Measurements of n-p correlations in the reaction of relativistic neon with uranium*

K. Frankel, W. Schimmerling, J.O. Rasmussen,
K.M. Crowe, J. Bistirlich, H. Bowman, O. Hashimoto,
D.L. Murphy, J. Ridout, J.P. Sullivan,+ and E. Yoo

Lawrence Berkeley Laboratory
University of California, Berkeley, CA 94720, USA

W.J. McDonald

University of Alberta, Edmonton, Canada

M. Salomon

University of British Columbia, Vancouver, B.C., Canada

and

J.-S. Xu

Fudan University, Shanghai, P.R. China

*This work was supported by the Director, Office of Energy Research, Division of Nuclear Physics of the Office of High Energy and Nuclear Physics of the U.S. Department of Energy under Contract DE-AC03-76SF00098 and the National Aeronautics and Space Administration.

+Current address: Cyclotron Institute, Texas A & M University, College Station, TX 77843, USA

Abstract

We report a preliminary measurement of coincident neutron-proton pairs emitted at 45° in the interaction of 400, 530, and 650 MeV/A neon beams incident on uranium. Charged particles were identified by time of flight and momentum, as determined in a magnetic spectrometer. Neutral particles were detected using a thick plastic scintillator, and their time of flight was measured between an entrance scintillator, triggered by a charged particle, and the neutron detector. At each beam energy, the calculated momentum correlation function for the neutron-proton pairs is enhanced near zero neutron-proton momentum difference by approximately one standard deviation over the expected value for no correlation. This enhancement is expected to occur as a consequence of the attractive final state interaction between the neutron and proton (i.e., virtual or "singlet" deuterons). The implications of these measurements are discussed.

Introduction

We have investigated the feasibility of observing virtual singlet deuterons (i.e., n-p pairs in the unbound spin singlet state), produced in relativistic heavy ion collisions, by measuring the momentum correlation between neutrons and protons detected in coincidence. The production of these singlet deuterons is of intrinsic interest and has been extensively studied at low energies. [1-3] In the case of relativistic heavy ion reactions, it may be possible to obtain information about spin ordering in the interaction region by measuring the ratio of triplet to singlet deuteron yield.

The singlet deuterons, the stable triplet deuteron, and other light fragments are thought to result from final state interactions of nucleons emerging from a highly excited interaction region. [4-6] Sato and Yazaki have generalized the coalescence model to include correlations of neutrons and protons. [7] In their calculation, the contribution of singlet and triplet spin states is weighted by the statistical factor 2S+1 that they would have in the absence of any ordering.

Spin ordering in the interaction region would occur in the presence of a phase change, such as has been predicted for pion condensation. Pion condensation of nuclear matter has been characterized as similar to an antiferromagnetic layered structure, [8-10] with antiparallel neutron and proton spins alternating in direction from layer to layer. Such an ordering would result in an altered ratio of formation of singlet and triplet states, and we propose the use of the singlet-to-triplet ratio as a test of such a phenomenon.

In the present work we have been limited by experimental constraints to the observation of momentum-correlated n-p pairs, since a measurement of deuteron yields in the same momentum range was beyond the capabilities of the available apparatus. We were able to find a correlation signal for n-p pairs with similar momenta that was well above the uncorrelated background. In the framework of the coalescence model it seems reasonable to assume that correlated n-p pairs in the triplet state emerge as bound deuterons and that deuteron breakup is negligible and, hence, that the majority of the observed correlated n-p pairs are due to virtual singlet deuterons. Such an assumption is justified, in part, by the agreement of observed neutron-to-proton inclusive cross-section ratios [11] with predictions based on counting the nucleons bound in observed fragments as part of the "primordial" nucleon spectrum. [12]

Experimental Arrangement

A scale diagram of the experimental arrangement is shown in Fig. 1. The neon beam was produced at the Lawrence Berkeley Laboratory Bevalac and extracted at energies of 425A, 557A, and 670A MeV. The beam particles lost an estimated 2-4 of their energy traversing various materials between the extraction point and the center of the target. A uranium target and a "dummy" target holder were used for various experimental tests. The data reported here were obtained with a 0.968 g cm^{-2} ^{238}U target.

The experimental arrangement for measuring and identifying charged particles consists of four sets of multiwire proportional chambers (MWPC1 to MWPC4) that determine the trajectory of a charged particle in the magnetic field of a magnet with entrance plane parallel to the beam line. Scintillators S_1 and S_2 at the entrance to the magnet, triggered in coincidence by a charged particle, provided a starting signal for two different time-of-flight (TOF) measurements. One of these measurements corresponded to the TOF of charged particles between S_1, S_2, and a "picket fence" of scintillation counters denoted A and B; the other measurement corresponded to the TOF of neutrons (and gamma rays) between S_1, S_2, and a 25.4 cm diam, 15 cm thick plastic scintillator N_1. A second neutron detector, N_2, was placed next to N_1, but shadowed by the magnet yoke, to sample accidental n-p coincidences produced by background neutrons. Charged-particle veto counters, V_1 and V_2, consisting of 6-mm thick plastic scintillators, were placed before N_1 and N_2.

The spectrometer was positioned to detect particles emitted at a laboratory angle of 45° (+6°,-8.4°), defined by scintillator S_2 and MWPC2; the neutron detector diameter subtended an angle of 2.5°. Typical charged-particle trajectories are shown in Fig. 1 for momenta of 400, 800, and 1200 MeV/c. At momenta above ~1 GeV/c, the momentum resolution for charged particles is 10 MeV/c. At lower momenta the resolution is limited by scattering in the wire chambers and intervening material and is estimated to be 4% at 500 MeV/c for protons.

The neutron detector had a TOF resolution of 0.9 nsec, as given by the full-width at half-maximum (FWHM) of the gamma-ray peak (obtained using a thick target for better statistics). The pulse height of signals produced in N_1 and N_2 was measured for every detected particle and calibrated against the light output produced with a ^{228}Th source [13]; events resulting in a light output greater than that expected for 7 MeV recoil protons were accepted. With this threshold the neutron detection efficiency of N_1 and N_2 was calculated to be ~16 for neutron momenta above 500 MeV/c, increasing to a maximum of ~24% at lower momenta down to ~250 MeV/c. The detector properties are tabulated in Table I.

The detectors were shielded from background events produced along the beam line by a lead wall extending beyond the magnet. Shielding against events produced in the beam dump ~8 m downstream from the target was also provided. As a consequence, background events, measured as a ratio of empty target holder to real target as well as spectra obtained by N_2, were negligible. A calculation of accidental coincidences caused by p-n knockout reactions in S_1S_2 yielded an effect at the 1% level.

Pulse heights in all scintillation counters, the TOF in the charged and neutral arm of the spectrometer, and the MWPC positions were recorded on magnetic tape with a PDP 11/45 computer-based data acquisition system [14]. The triggering logic was given by S_1 and S_2 in coincidence with at least one pair of the A-B scintillators and with either N_1 or N_2 and in anticoincidence with V_1 and V_2.

The beam intensity was monitored with two calibrated ionization chambers and a scintillator telescope. Beam rates were kept below 10^7 particles/pulse for the final data, to keep accidental n-p coincidences low.

Data Analysis

For charged particles the momenta and direction cosines of the vector momentum were obtained from the MWPC trajectories and the measured magnetic field data; the momentum of neutrons was obtained from the TOF. The charged particles at 45° consist[5] mainly of p, d, ^3H, ^3He, and ^4He. The spectrometer acceptance is strongly biased against detection of the relatively slow, short-range isotopes corresponding to the same rigidity as the accepted hydrogen isotopes. The simultaneous TOF and momentum information was used to separate protons and deuterons. Figure 2 is a scatter plot of the observed charged-particle events as a function of TOF and momentum. Three regions can be clearly distinguished, corresponding to the values calculated for the hydrogen isotopes. To identify protons and deuterons boundaries defined by the line segments A–F were used as shown in Fig. 2. The singles spectra are shown in Fig. 3. The upper and lower boundaries of these spectra include the effects of the spectrometer acceptance cutoff. At the high end, the acceptance was limited by the magnetic field of the spectrometer and at the low end by the minimum range of the particle required to produce an acceptable signal in a detector of A or B.

Figure 4 shows a scatter plot and a computer generated contour plot (in relative units) of the events in the momentum plane p_n and p_p. The horizontal angle increment accepted corresponds to almost twice the neutron detector angle increment, and it is centered at a mean angle of 43.5°.

To show the correlation between the np pairs, we have calculated the correlation function in the manner used by Zajc for 2-pion correlations.[14] The spectrometer has peaked distributions for the proton spectra. Uncorrelated n–p events may show an apparent correlation, even though the neutron acceptance and the emission cross sections are relatively flat [4,11]. We correct for possible bias by taking the ratio of correlated events to correlations generated by sampling neutrons and protons from different events;

$$1 + R \equiv C = (N - 1)S_{np}/S_{mix} \quad , \tag{1}$$

where $1 + R \equiv C$ is the correlation function, and where S_{np} is the number of np pairs (same event) whose momentum difference $\Delta p = \vec{p}_n - \vec{p}_p$ falls into a given bin. S_{mix} is based on a population consisting of a proton, p_p from one event and neutrons with momentum p_n from all other events with the same Δp. The factor N − 1 arises because there are N events for S_{np} and N(N − 1) "pseudoevents" for S_{mix}. The measured S_{mix} is also a function of R, and Eq. (1) would normally be iterated to remove this dependence [14]. In our case, the statistical fluctuations associated with the small number of events were too large to result in a convergent iteration.

The proton momentum resolution varies between 5 and 15 MeV/c as the proton momentum decreases from 1000 to 250 MeV/c, whereas the neutron momentum resolution has the opposite behavior, varying between 70 and 5 MeV/c in the same momentum range. On this basis, the bin width chosen was Δp = 25 MeV/c, which is equal to the expected resolution in the region around 500 MeV/c, where most events are detected.

The correlation functions are plotted in Figs. 5a,b, and c for the data sets corresponding to each of the incident beam energies. The figures represent projection over a broad proton angle cut of 36.6°– 51°, though most significant events lie between 39° and 46°, as discussed below.

At all beam energies the bin around zero Δp has the most events and usually the highest correlation function. The correlation function falls off on either side with about the momentum resolution intrinsic to the experiment. The side peaks have few events and are considerably less than a standard deviation above 1. The central peak rises to values of 1.34 to 1.63, at all beam energies being about one standard deviation above unity (i.e., above the value expected for no correlation). Off-peak the correlation function is unity within statistics. When we noted side peaks, we at first thought we might be able to measure the n-p pair breakup at the nuclear surface relative to breakup after full Coulomb acceleration. In the former case the final proton energy would exceed the neutron energy by the Coulomb potential at breakup, while in the latter case the correlated proton and neutron energies should be the same. The nominal surface Coulomb energy for uranium is ~15 MeV and for the fused uranium-neon ~16 MeV. An extra 15 MeV applied to a mean proton energy of 130 MeV in this experiment will give a momentum shift of 33 MeV/c. Although the main peak in Figs. 5a,b, and c seems slightly (~15 MeV/c) shifted, our knowledge of the true zero is not this accurate. Observation of correlation peak shape and absolute shifts could help to determine the range of distances over which n-p pair breakup occurs, but better momentum resolution and statistics are needed.

The apparent width in angle of the correlation function is of the order of 6 degrees, which for the most probable momentum gives an angular width of ~50 MeV/c, neglecting corrections due to possible small angle neutron scattering into the detector. This apparent width is consistent with that expected on the basis of the neutron detection angle and the smearing of the proton emission angle by multiple scattering in the uranium target and the two entrance scintillators. (The proton multiple scattering angle varies between 2.5° and 0.5°, and is calculated as 1.1° at the mean momentum of 500 MeV/c.)

Table II shows the correlation functions for the three different beam energies. Column 2 is the average over all non-central bins, i.e., the baseline for normalization. In column 3 we give the value of the central bin (same as figures). In column 4 the normalized correlation function, i.e.

ratio of column 3 to column 2 is given. Column 4 may be the best measure of the true correlation function, since the base line of column 2 should be unity, or uncorrelated. The three measurements of positive correlation, are approximately 1 standard deviation above unity.

Discussion

Sato and Yazaki [6,7] have developed the theory of two-nucleon correlations with the density matrix formalism. Their Fig. 4 of Ref. 7 shows explicitly the n-p correlation expected in a heavy-ion collision with fireball radius of 3 fm and with four different values of their diffusion length parameter λ. They state that the n-p correlation is given approximately by three-fourths of the n-n correlation. These correlation functions are slightly anisotropic and sharply peaked at zero momentum difference, falling to half their central values by about 15 MeV/c. Their narrow predicted widths are consistent with a correlation within the first bin of 25 MeV/c width. Future experiments clearly should improve on our neutron momentum resolution, either by sharper timing or longer flight paths. Also, many neutron detectors or large position-sensitive detectors should be used. The "singlet-to-triplet" (unbound-to-bound) deuteron ratio cannot be estimated reliably from the data obtained by this experiment. We believe we have demonstrated the feasibility of n-p correlation experiments with relativistic heavy-ion beams, and we have shown that the correlation is sharper than ~25 MeV/c, consistent with Sato-Yazaki theory. Future experiments must be carried out with better resolution and statistics in order to test this theory and to determine whether an anisotropy exists.

Acknowledgements

We express appreciation to Fred Lothrop and the crew of the Bevalac for making these experiments possible.

We thank T. Humanic for helpful conversations.

W.J. McDonald would like to acknowledge J. O. Rasmussen and W. Schimmerling for their hospitality and support and to the National Sciences and Engineering Research Council of Canada for support.

This work was supported by the Director, Office of Energy Research, Division of Nuclear Physics of the Office of High Energy and Nuclear Physics, and also in part by the Director, Office of Energy, Health, and Environmental Research, of the U.S. Department of Energy under Contract DE-AC03-76SF00098 and by the National Aeronautics and Space Administration.

References

1. Cohen, B.L., May, E.C., O'Keefe, T.M., and Fink, C.L., Phys. Rev. 179, 962 (1969).
2. van der Weerd, J.C., Canada, T.R., Fink, C.L., and Cohen, B.L., Phys. Rev. C3, 66 (1971).
3. Burq, J.P., Cabrillat, J.C., Chemarin, M., Ille, B., and Nicolai, G., Nucl. Phys. 179A, 371 (1972).
4. Gosset, J., Gutbrod, H.H., Meyer, W.G., Poskanzer, A.M., Sandoval, A., Stock, R., and Westfall, G.D., Phys. Rev. C16, 629 (1977).
5. Nagamiya, S., Lemaire, M.-C., Moeller, E., Schnetzer, S., Shapiro, G., Steiner, H., and Tanihata, I., Phys. Rev. C24, 971 (1981).
6. Sato, H. and Yazaki, K., Phys. Lett. 98B, 153 (1981).
7. Sato, H. and Yazaki, K., Proc. Hakone Seminar on "High Energy Nuclear Interactions and Properties of Dense Nuclear Matter" (K. Nakai and A.S. Goldhaber, eds.), Japan Society for the Promotion of Science and U.S. National Science Foundation, Hakone, Japan, 1980, Vol. I, p. 340.
8. Takatsuka, T., Tamiya, K., Tatsumi, T., and Tamagaki, R., Prog. Theor. Phys. 59, 1933 (1978).
9. Tamiya, K., and Tamagaki, R., Prog. Theor. Phys. 60, 1753 (1978).
10. Ericson, M., and Deloreme, T., Phys. Lett. 76B, 1820 (1978).
11. Schimmerling, W., Kast, J.W., Ortendahl, D., Madey, R., Cecil, R.A., Anderson, B.D., and Baldwin, A.R., Phys. Rev. Lett. 43, 1985 (1979).
12. Stevenson, J.D., Phys. Rev. Lett. 45, 1773 (1980).
13. Cecil, R.A., Anderson, B.D., and Madey, R., Nucl. Instr. Meth. 161, 439 (1979).

14. Zajc, W., Bistirlich, J. A., Bossingham, R. R., Bowman, H. R., Clawson, C. W., Crowe, K. M., Frankel, K. A., Ingersoll, J. G., Kurck, J. M., Martoff, C. J., Murphy, D. L., Rasmussen, J. O., Sullivan, J. P., Yoo, E., Hashimoto, O., Koike, M., McDonald, W. J., Miller, J. P., and Truol, P., Phys. Rev. C 29, 2173 (1984).

Table I.

Experimental Parameters

1. Incident Beam:

   Neon at 650, 530, 400 AMeV

2. Target:

   ^{238}U (0.968 g/cm^2)

3. Neutral Detector:

   Solid Angle: 1.4 msr

   Neutron Efficiency: 16% above 500 MeV/c

   Pulse-height Threshold: 7 MeV protons

   TOF Resolution (FWHM Gamma Peak): 0.9 ns

   $\Delta p/p$ (0.25–1.0 GeV/c): 1–7

4. Charged Particle Detector:

   Solid angle: 30 msr

   Max. Proton Efficiency: ~75%

   Max. Deuteron Efficiency: ~50%

   TOF Resolution: 0.9 ns

   $\Delta p/p$ (1.0–0.25 GeV/c): 1–6%

Table II.

Averaged Values of Correlation Function

Beam Energy A MeV	$\langle 1 + R \rangle_{\Delta P > 25\ MeV/c}$ Non-Central Bins	$\langle 1 + R \rangle_{25\ MeV/c}$ Central Bin	$\langle 1 + R \rangle_{norm}$
400	0.75 ± 0.18	1.51 ± 0.46	2.02 ± 0.78
530	0.81 ± 0.12	1.16 ± 0.24	1.44 ± 0.37
650	0.79 ± 0.12	1.22 ± 0.26	1.54 ± 0.40

Figure Legends

Fig. 1. Schematic layout of JANUS spectrometer system for the n-p correlation experiment. Magnet and detector sizes are to scale, but the positions are only approximately to scale. Trajectories for protons of three different momenta are shown. Time of flight is determined between coincident scintillators S_1-S_2 and coincident scintillators A-B for charged particles and between S_1-S_2 and N_1 for neutron particles. The four multiwire proportional counters MWPC1-4 define the charged particle trajectories through the magnet. V_1 and V_2 are thin scintillators used to veto events with a charged particle incident on N_1 and N_2.

Fig. 2. Scatter plot of charged particle time of flight vs their momentum. Protons and deuterons were assigned to the regions labelled "p" and "d", respectively, by inspection, and line segments A-F were drawn by hand to demarcate the separate regions.

Fig. 3. Spectrum of charged particles separated as shown in Fig. 2, plotted vs total momentum. Notice that the momentum of the detected deuterons corresponds to about twice the momentum of each nucleon, so a comparison between singlet (np pairs) and triplet deuterons at the same momentum was not possible. The peaking of the spectra is an artifact introduced by the acceptance cutoff of the spectrometer.

Fig. 4a.b Scatter plot and contour plot (in relative units) of neutron momentum vs proton momentum for momenta between 300 and 1000 MeV/c. The data obtained with all three beam energies have been pooled to make the correlation pattern recognizable by eye.

Fig. 5a–c. Correlation functions histogram for data obtained at beam energies of ~400, ~530, and ~650 AMeV, as a function of the momentum difference between the neutron and proton. The bin width was Δp = 25 MeV/c in all cases. The statistical standard deviation is shown by dashes above and below each histogram/bin, and the number of events in each bin is written at the top.

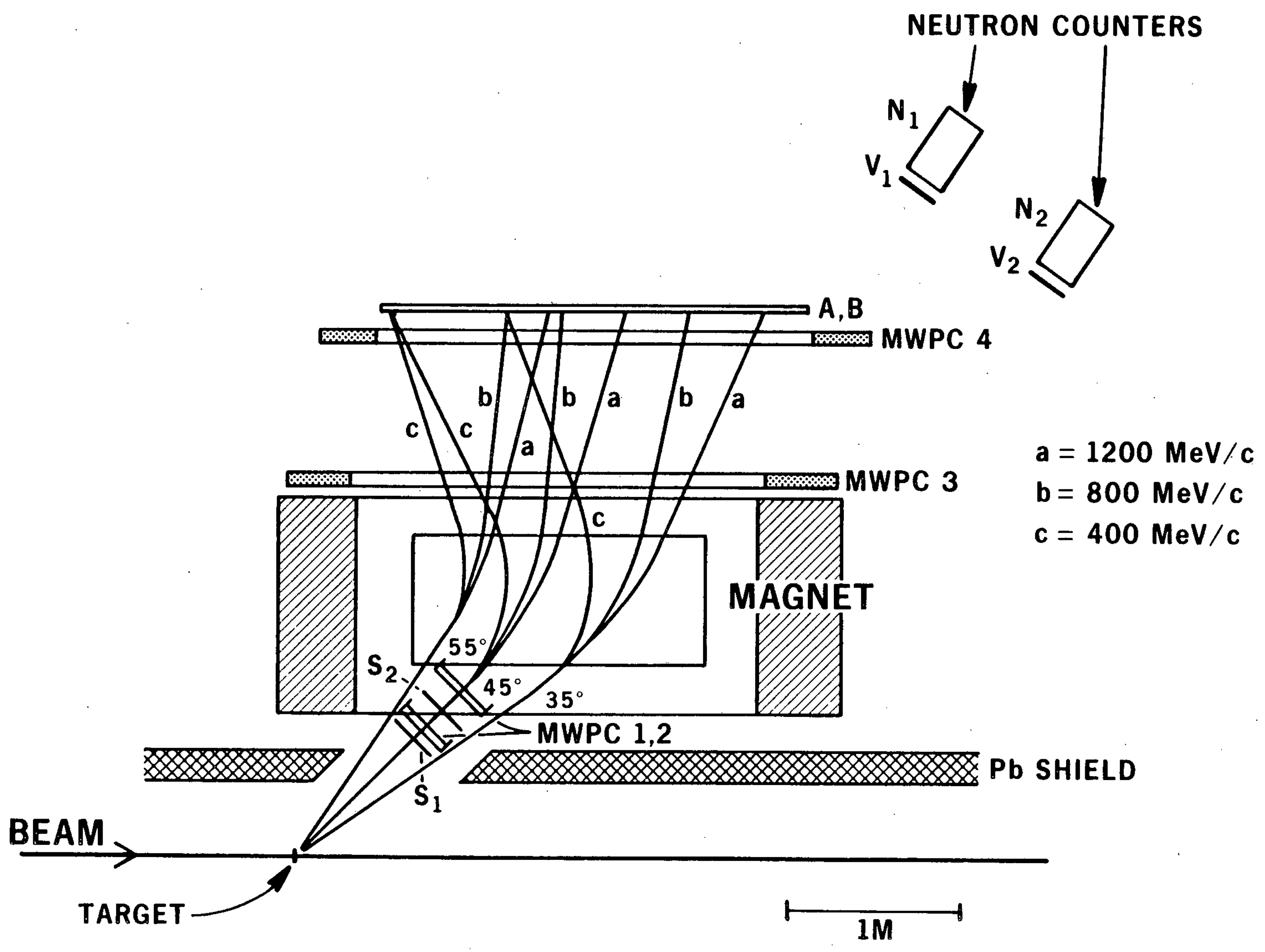

XBL 835-9543

Fig. 1

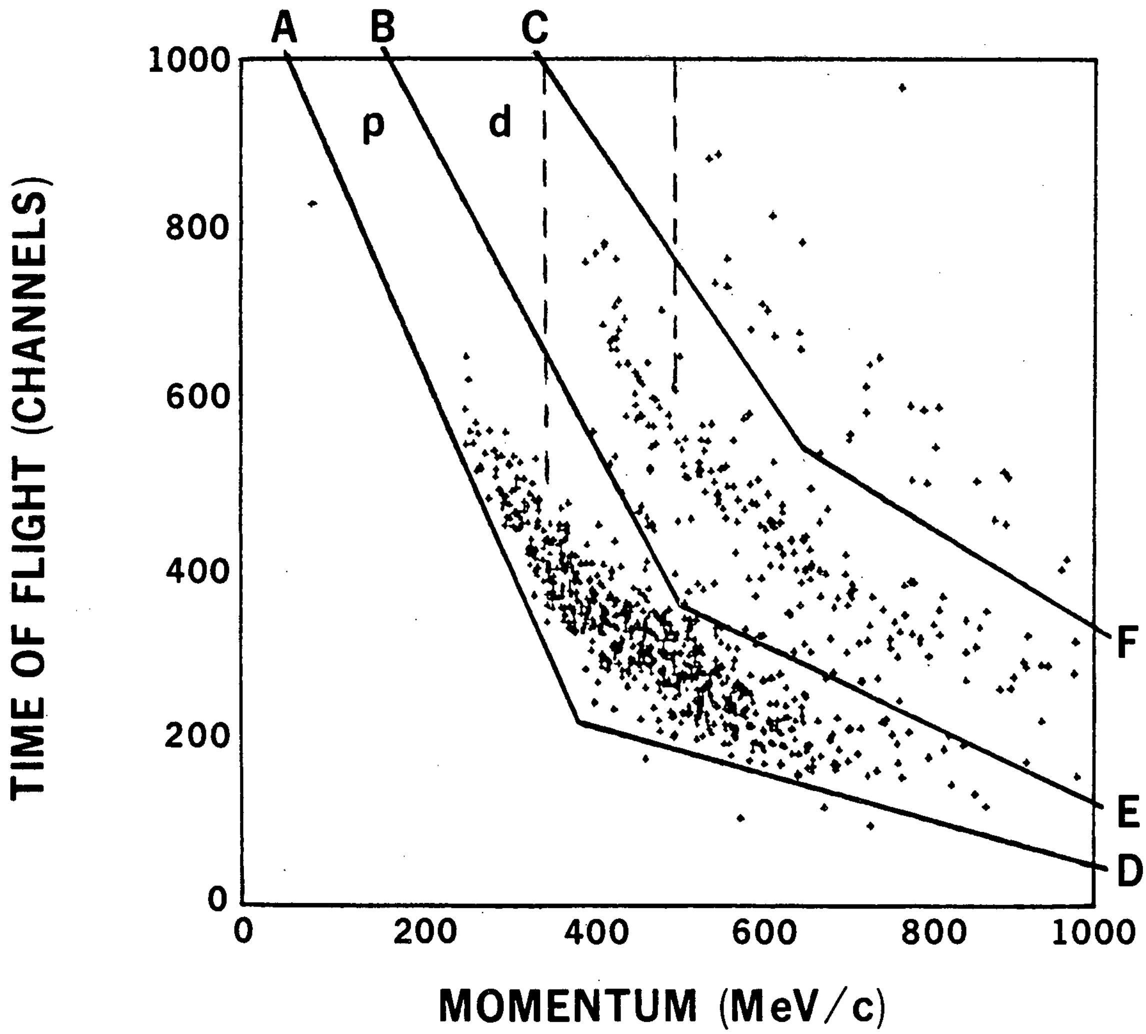

XBL 835-9542

Fig. 2

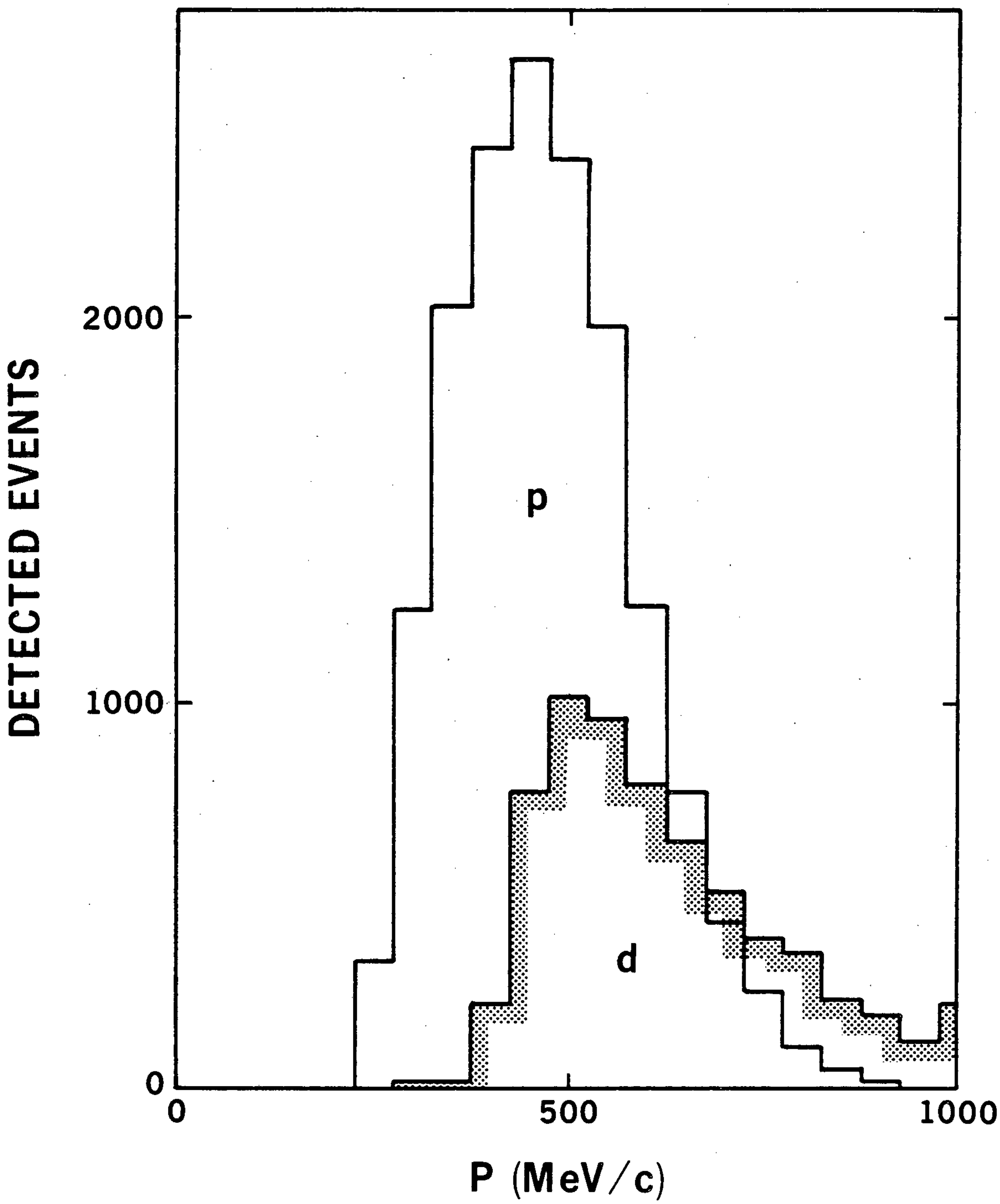

XBL 835-9545

Fig. 3

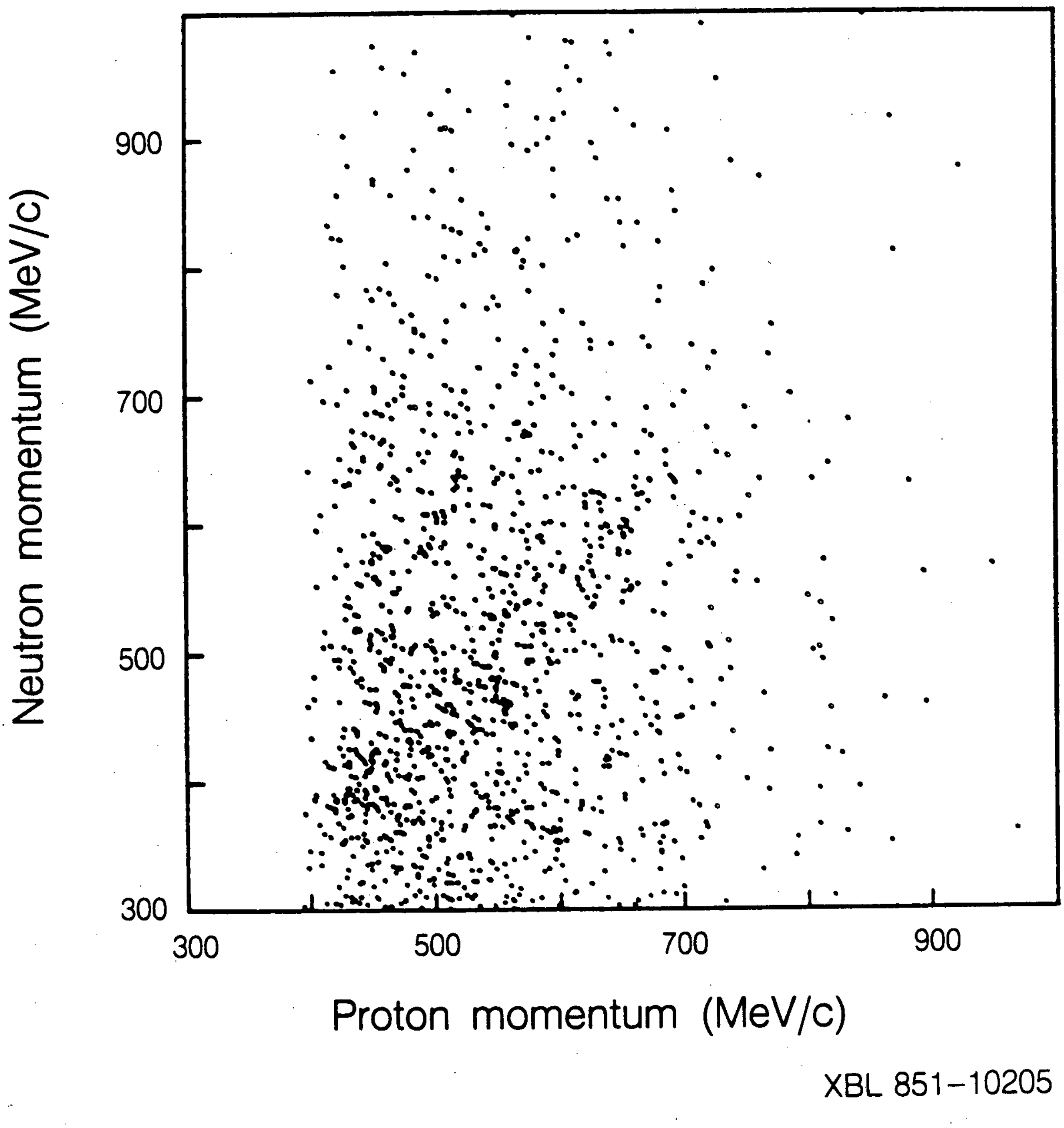
Neutron momentum (MeV/c)
900
700
500
300
300
500
700
900
Proton momentum (MeV/c)
XBL 851-10205

Fig. 4a

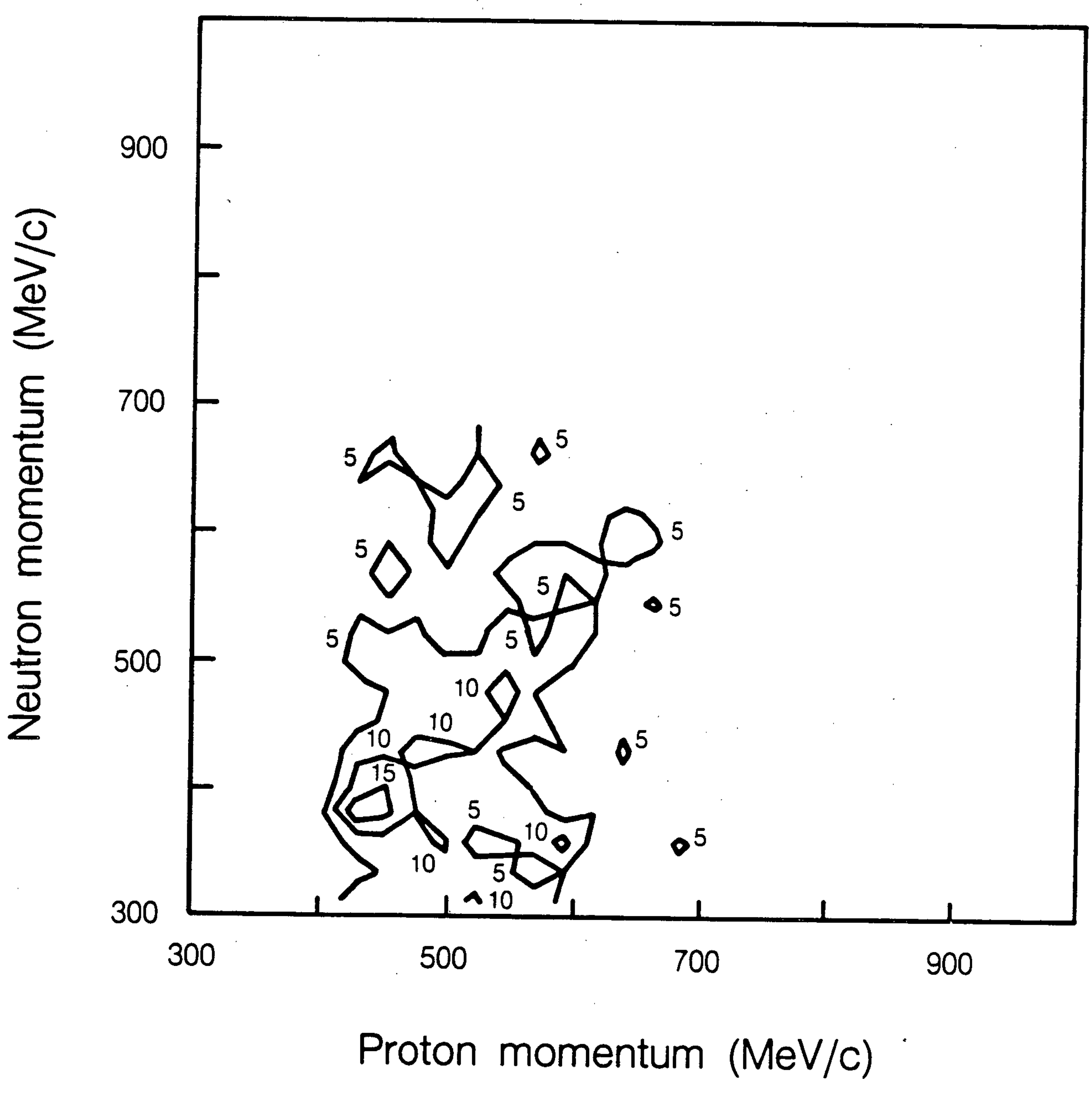

XBL 851-10204

Fig. 4b

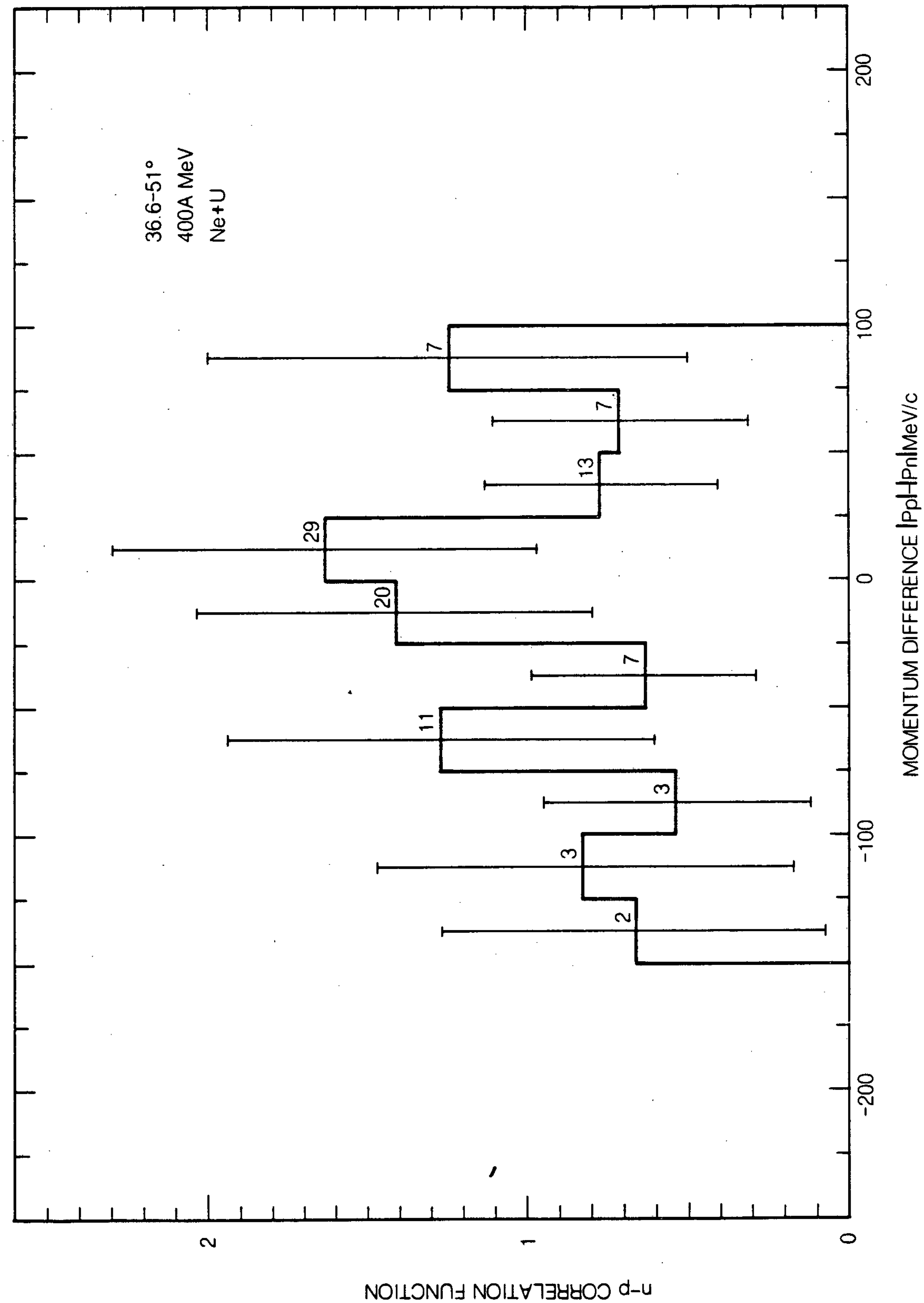

XBL 837-439

Fig. 5a

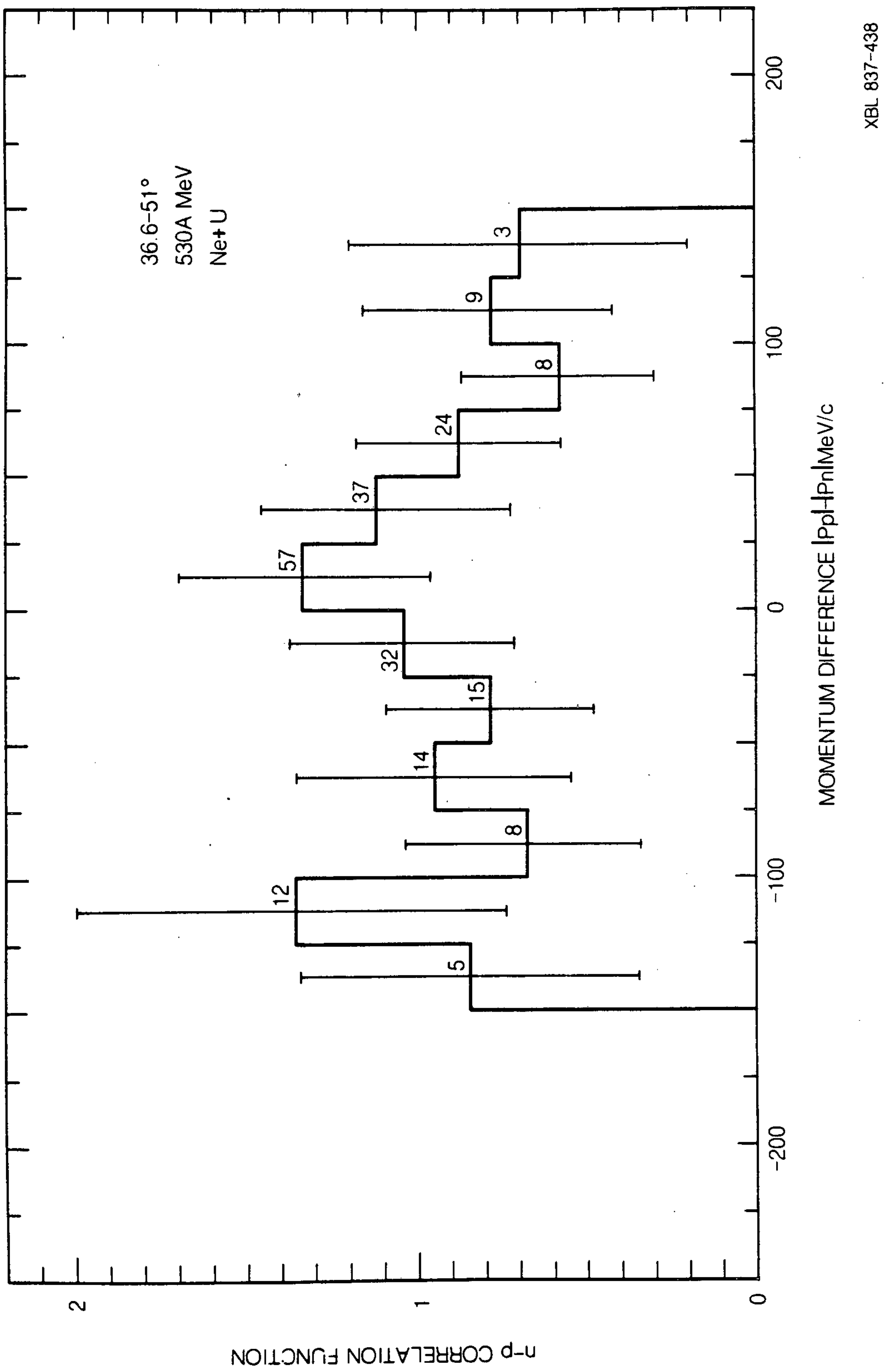

36.6–51°
530A MeV
Ne+U
MOMENTUM DIFFERENCE |Pp|–|Pn| MeV/c
n–p CORRELATION FUNCTION
XBL 837-438

Fig. 5b

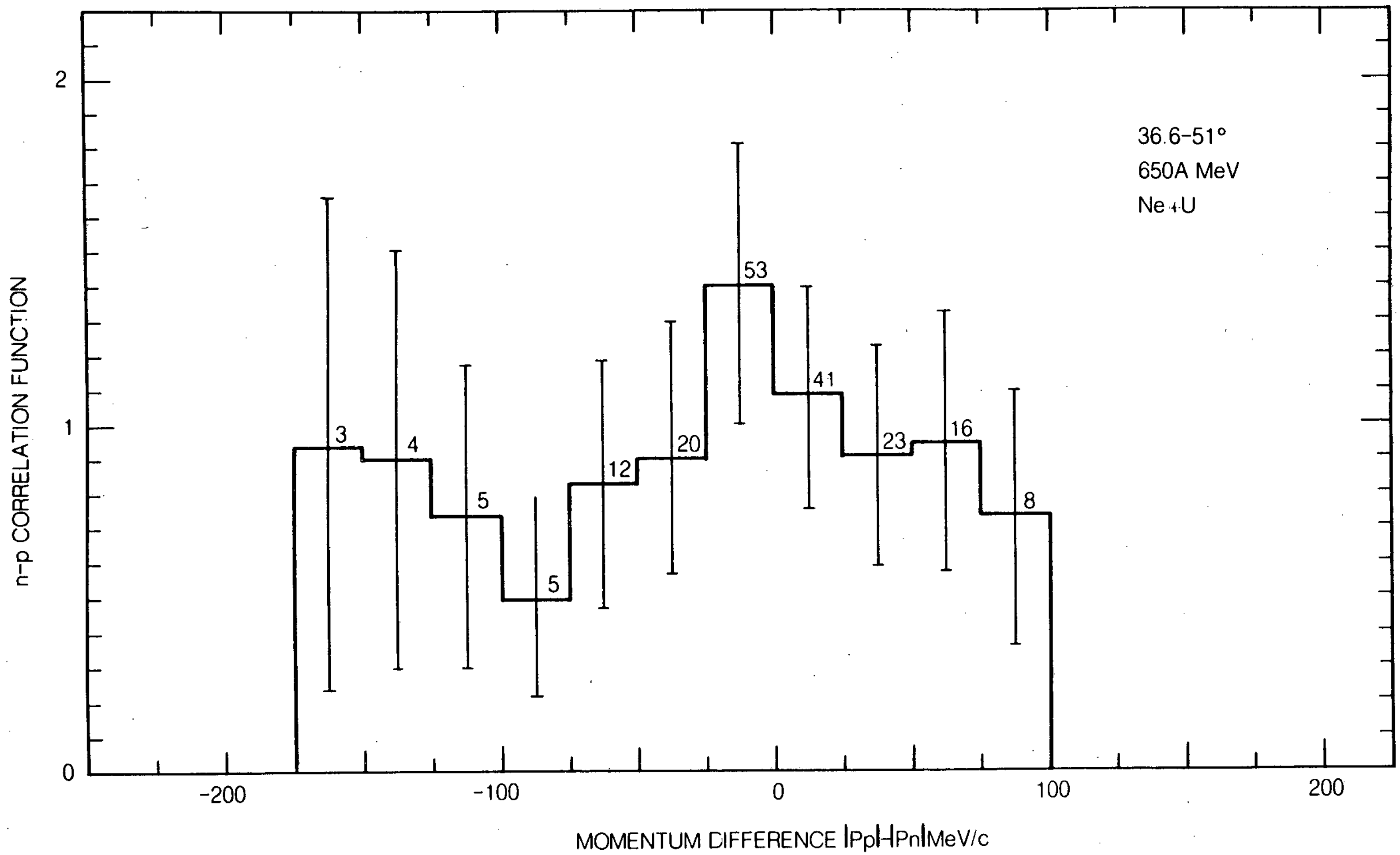

XBL 837-440

Fig. 5c

LAWRENCE BERKELEY LABORATORY
TECHNICAL INFORMATION DEPARTMENT
UNIVERSITY OF CALIFORNIA
BERKELEY, CALIFORNIA 94720